

Equilibrium Thermodynamics of a Physiologically-Relevant Heme–Protein Complex[†]

Xuming Wang and Gary J. Pielak*

Department of Chemistry, University of North Carolina at Chapel Hill, Chapel Hill, North Carolina 27599-3290

Received August 26, 1999; Revised Manuscript Received October 6, 1999

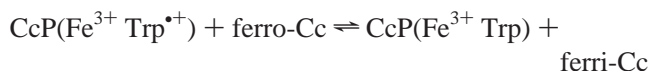
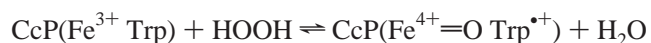
ABSTRACT: We used isothermal titration calorimetry to study the equilibrium thermodynamics for formation of the physiologically-relevant redox protein complex between yeast ferricytochrome *c* and yeast ferricytochrome *c* peroxidase. A 1:1 binding stoichiometry was observed, and the binding free energies agree with results from other techniques. The binding is either enthalpy- or entropy-driven depending on the conditions, and the heat capacity change upon binding is negative. Increasing the ionic strength destabilizes the complex, and both the binding enthalpy and entropy increase. Increasing the temperature stabilizes the complex, indicating a positive van't Hoff binding enthalpy, yet the calorimetric binding enthalpy is negative (−1.4 to −6.2 kcal mol^{−1}). We suggest that this discrepancy is caused by solvent reorganization in an intermediate state. The measured enthalpy and heat capacity changes are in reasonable agreement with the values estimated from the surface area change upon complex formation. These results are compared to those for formation of the horse ferricytochrome *c*/yeast ferricytochrome *c* peroxidase complex. The results suggest that the crystal and solution structures for the yeast complex are the same, while the crystal and solution structures for horse cytochrome *c*/yeast cytochrome *c* peroxidase are different.

Iso-1-cytochrome *c* (Cc)¹ from the yeast *Saccharomyces cerevisiae* and Cc peroxidase from *S. cerevisiae* (CcP) are physiological redox partners. Cc, a 12.5 kDa single-domain protein with a covalently bound heme *c*, is the penultimate electron-transfer protein of the eukaryotic respiratory chain whose main function is to accept electrons from Cc reductase and donate them to Cc oxidase. CcP is a 35 kDa monomer with a noncovalently bound heme *c*. Although the physiological function of CcP is obscure [deletion of the CcP gene does not affect the growth rate of yeast under laboratory conditions (1)], its complex with Cc is an important model for protein–protein binding in general and electron-transfer complexes in particular. High-resolution structures are available for both proteins alone and for the complexes of horse Cc (hCc) with CcP and yeast Cc (yCc) with CcP (2–8).

As shown in Scheme 1, CcP undergoes a two-electron oxidation by a peroxide to form a radical-containing intermediate, compound I. Compound I is reduced back to the resting state by two ferrocytochrome *c* molecules in two consecutive one-electron steps.

In 1960, Beetlestone found that ferri-Cc is a competitive inhibitor of ferro-Cc in CcP-catalyzed reactions (9). Since then, many techniques have been used to study complex formation between CcP and cytochromes *c* from different species. These techniques include sedimentation velocity (10), analytical ultracentrifugation (11), gel chromatography

Scheme 1



(10, 12, 13), electronic absorption spectroscopy (14), nuclear magnetic resonance spectroscopy (15–18), fluorescence quenching (13, 19, 20), potentiometric titration (21), and isothermal titration calorimetry (ITC) (22, 23).

Most researchers report 1:1 binding of Cc to CcP in solution, and this stoichiometry is observed in the crystal structure of the complex (8). The binding constant, *K*_B, decreases with increasing ionic strength, indicating that electrostatic interactions contribute to binding (21, 24). This observation is also consistent with the crystal structure, which shows that the binding interface comprises both electrostatic interactions and buried nonpolar surface.

In 1977, Kang et al. (12) found that CcP can bind more than one Cc. More recently, Hoffman and co-workers proposed a model with a 2:1 binding ratio for the complex involving Zn-substituted -Cc or -CcP (24–26). For the yeast ferri-Cc/CcP complex, the binding free energies, Δ*G*_B, for the high- and low-affinity binding sites are ≤−10.0 and ≥−5.5 kcal mol^{−1}, respectively, at pH 6 and 25 °C in 1–10 mM potassium phosphate buffer. At buffer concentration >50 mM, the low-affinity binding site is not detected. Data from potentiometric titration of the yCc/CcP complex (21) are also consistent with a two-site model. At <100 mM ionic strength and between pH 6.0 and pH 7.75, Δ*G*_B ranges from

[†] This work was supported by NIH Grant GM42501.

* To whom correspondence should be addressed. Phone: (919) 966-3671. FAX: (919) 966-3675. E-mail: gary_pielak@unc.edu.

¹ Abbreviations: Cc, cytochrome *c*; CcP, cytochrome *c* peroxidase from the yeast *Saccharomyces cerevisiae*; DMG, dimethylglutaric acid; hCc, horse Cc; ITC, isothermal titration calorimetry; SASA, solvent-accessible surface area; yCc, iso-1-Cc from the yeast *S. cerevisiae*.

−6.9 to −9.1 kcal mol^{−1} for the high-affinity site and from >−4.1 to −4.7 kcal mol^{−1} for the low-affinity site. At ionic strengths >100 mM, the low-affinity site is not detected.

Isothermal titration calorimetry provides a direct measure of binding enthalpy, ΔH_B , but, until now, ITC has only been applied to the horse ferri-Cc/yeast ferri-CcP complex (22). To gain information on the formation of the physiologically-relevant complex, we studied the reaction between yCc and CcP and present thermodynamic data as a function of pH, temperature, ionic strength, Cc oxidation state, and buffer.

EXPERIMENTAL PROCEDURES

Nomenclature. Unless stated otherwise, Cc and CcP refer to the ferri forms of these proteins. The C102T variant of yCc was used throughout this study. This mutation eliminates dimerization, making the protein more amenable to biophysical studies, but does not change the protein's structure or function (3, 27, 28).

Protein Expression and Purification. yCc was purified from yeast as described by Willie et al. (29). Recombinant yeast CcP was expressed and purified from *Escherichia coli* by using a modified version of a previously published protocol (30). The plasmid containing the CcP gene was a gift from Thomas Poulos of the University of California at Irvine. For each preparation, the plasmid was freshly transformed to *E. coli* strain BL21DE3 (Stratagene, La Jolla, CA). Cells were lysed by using the freeze–thaw method. The ratio of the absorbance at 408 nm to that at 280 nm ranged between 1.26 and 1.33, showing that CcP has a 5-coordinate high-spin heme (31). Aliquots of CcP crystals were stored in deionized–distilled water at −80 °C and dissolved in buffer before use.

ITC. Experiments were performed on a Microcal MCS–ITC (Northampton, MA). The buffers, dimethylglutaric acid (DMG), cacodylic acid, and sodium 2-(*N*-morpholino)-ethanesulfonic acid (MES), were from Sigma (St. Louis, MO). The pHs of DMG and cacodylate solutions were adjusted with NaOH. MES solutions were made from the hemisodium salt, and the pH was adjusted with HCl solution. Unless otherwise stated, the buffer concentration was 50 mM. To study the ionic strength dependence, 10 mM DMG was used, and the ionic strength was adjusted with NaCl. Before each experiment, Cc and CcP were dialyzed (Slide-A-Lyzer membrane, 2000 and 7000 MWCO, Pierce, Rockford, IL) against buffer in the same beaker for >36 h with three buffer changes (buffer-volume:sample-volume >100). For experiments with ferro-Cc, dithiothreitol was added to all buffers to a final concentration of 1 mM. After dialysis, the protein concentrations were measured by UV–vis spectrophotometry. Cc concentration was determined by averaging the absorbance measurements at five redox isobestic points, 339, 410, 434, 504, and 526.5 nm, using extinction coefficients of 20.9, 106.1, 22.7, 6.6, and 11.0 mM^{−1} cm^{−1}, respectively. CcP concentration was determined at 408 nm by using an extinction coefficient of 102 mM^{−1} cm^{−1} (30). Cc concentrations were >1 mM, and CcP concentrations were adjusted with buffer to 30–100 μM.

Cc was placed in the 250 μL syringe. The syringe was rotated at 400 rpm for the duration of each experiment. The injection volume was 4–10 μL depending on the protein concentrations and was constant for each experiment. The

time between injections was 480 s. The reference cell contained deionized–distilled water. The water bath temperature was maintained at 5 °C below the temperature of the sample cell. The heat of yCc dilution was determined by titrating yCc into buffer, and subtracted from the data before analysis.

We processed the data with the ITC module within Origin 4.0 (Microcal Software, Northampton, MA). Base line and start- and end-points for integration of each peak were adjusted manually. Integrated data were corrected for the heat of dilution, and the first data point was removed before fitting. A nonlinear fitting model with the Marquardt algorithm (32) was used. One- and two-site models were tested.

Surface Area Changes. Polar and nonpolar solvent-accessible surface area (SASA) changes were calculated by using the program GEOPOL (33). Structures for the yCc/CcP and hCc/CcP complexes (8) were obtained from the Brookhaven Protein Data Bank (2PCC and 2PCB, respectively). The van der Waals radii of amino acid atoms were from the work of Lee and Richards (34). Heme atom radii were 1.700 Å for all nitrogen and non-methyl carbon atoms, 2.000 Å for methyl carbon atoms, and 1.500 Å for propionate oxygen atoms. Carbon atoms were treated as nonpolar, and nitrogen and oxygen atoms were treated as polar (35). For both the yCc/CcP and hCc/CcP complexes, the A and B chains of the respective crystal structures were used for SASA calculation.

RESULTS

To obtain accurate thermodynamic parameters from ITC data, the product of macromolecule concentration in the sample cell and equilibrium binding constant should be between 1 and 10³ (36). This condition was fulfilled by using CcP concentrations in the 30–100 μM range. Representative ITC data are shown in Figure 1. The ΔG_B and ΔH_B values and the stoichiometry (*N*), shown in Table 1, were obtained by fitting data to a one-site model. The binding entropy, ΔS_B , values were obtained by using the Gibbs equation: $\Delta G_B = \Delta H_B - T\Delta S_B$.

pH. Experiments were performed at pH 6.0, pH 6.5, and pH 7.0 in 50 mM DMG buffer [*pK_a* = 3.7 and 6.2, (37)]. As shown in Table 1, ΔG_B increases with increasing pH, consistent with the potentiometric data of Mauk et al. (21). Both ΔH_B and ΔS_B favor binding, except at pH 7.0, where ΔS_B is unfavorable.

Temperature. Binding was investigated at five temperatures from 6 to 25 °C at pH 6.0 (Table 1). With increasing temperature, ΔG_B , ΔH_B , and ΔS_B decrease. At room temperature, the binding is more enthalpy-driven while at low temperature it is more entropy-driven. Linear least-squares fitting of the temperature dependence data in Table 1 yields a ΔC_p of -216 ± 62 cal mol^{−1} K^{−1}, where the uncertainty is the standard deviation of the best fit slope.

Ionic Strength. To investigate the ionic strength dependence, ITC experiments were performed at 25 °C in 10 mM DMG, pH 6.0, with added NaCl. The increase in ΔG_B with increasing ionic strength (Table 1) is the result of unfavorable changes in ΔH_B . ΔS_B becomes more favorable with increasing ionic strength. At 140 mM NaCl, the heat released from each injection is too small to be detected.

Table 1: Thermodynamic Parameters of yCc/CcP Binding Obtained from ITC Experiments^a

	N^b	ΔG_B	ΔH_B	$-T\Delta S_B$
pH				
6.0 (5)	0.97 ± 0.02	-8.1 ± 0.1	-6.2 ± 0.3	-1.9 ± 0.4
6.5 (4)	1.18 ± 0.11	-7.7 ± 0.1	-6.2 ± 0.4	-1.5 ± 0.4
7.0 (4)	1.09 ± 0.06	-7.4 ± 0.02	-7.8 ± 0.3	0.4 ± 0.3
temp (°C)				
6 (3)	0.70 ± 0.05	-7.4 ± 0.3	-1.4 ± 0.1	-6.0 ± 0.3
10 (3)	0.91 ± 0.07	-7.6 ± 0.2	-2.2 ± 0.2	-5.4 ± 0.4
15 (4)	0.79 ± 0.03	-7.8 ± 0.3	-2.8 ± 0.2	-5.0 ± 0.5
20 (3)	0.86 ± 0.04	-7.7 ± 0.3	-2.9 ± 0.1	-4.7 ± 0.2
25 (5)	0.97 ± 0.02	-8.1 ± 0.1	-6.2 ± 0.3	-1.9 ± 0.4
ionic strength ^c (mM)				
4 (4)	0.87 ± 0.05	-10.9 ± 0.4	-8.6 ± 0.9	-2.7 ± 0.8
14 (5)	0.89 ± 0.05	-9.9 ± 0.7	-6.6 ± 0.7	-3.3 ± 1.3
44 (5)	1.02 ± 0.02	-9.3 ± 0.4	-4.7 ± 0.1	-4.6 ± 0.4
94 (5)	0.97 ± 0.05	-8.1 ± 0.3	-2.4 ± 0.1	-5.7 ± 0.4
144 (2) ^d	—	> -4.0	$-0.5-0$	> -4.0
ferro-Cc (2)	1.14 ± 0.09	-7.1 ± 0.0	-3.1 ± 0.6	-4.0 ± 0.6

^a Experiments were performed at pH 6.0, 25 °C, in 50 mM DMG except as indicated. Units for ΔG_B , ΔH_B , and $-T\Delta S_B$ are kcal mol⁻¹. Uncertainties are the standard deviation of the mean for the number of experiments given in parentheses. ^b Binding ratio of Cc to CcP. ^c Buffers are 10 mM DMG with added NaCl of 0, 10, 40, 90, 140 mM. ^d Signal too weak to give precise parameters.

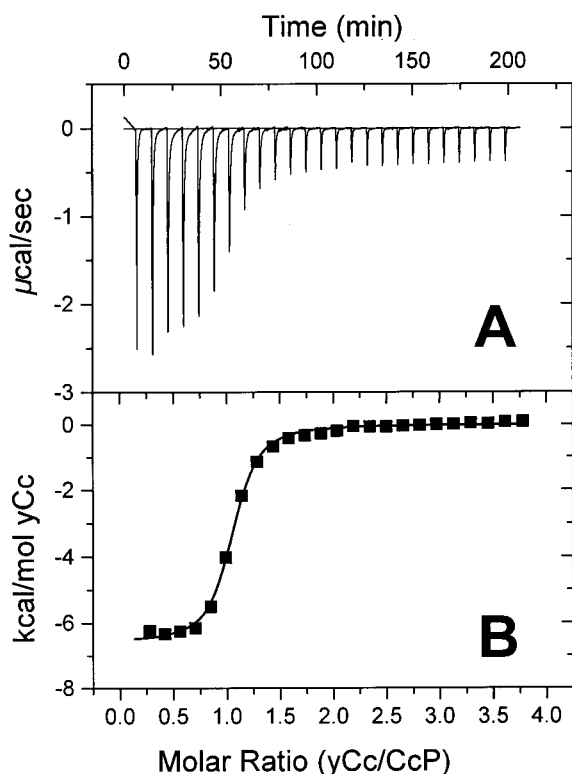


FIGURE 1: Binding of Cc to CcP at 25 °C, in 50 mM DMG, pH 6.0. The concentrations of Cc and CcP were 1.69 and 90.8 μ M, respectively. Injection volumes were 10 μ L. (A) Raw data after base line correction. (B) Integrated data corrected for heat of dilution of Cc. Solid squares, integrated data; solid line, best-fit by using a 1:1 binding model. The fit yields a ΔH_B of -6608 ± 65 cal mol⁻¹, a K_B of $(7.5 \pm 0.7) \times 10^5$, and a stoichiometry of 1.00 ± 0.01 Cc to CcP.

Buffer. ΔH_B obtained from ITC includes all the enthalpy changes from processes that occur in the system, not only the enthalpy change from the intrinsic binding reaction. One of the other processes is the coupling of buffer ionization to the uptake or release of protons upon complex formation:

$$\Delta H_B = \Delta H_B' + n \times \Delta H_{\text{ion}} \quad (1)$$

where $\Delta H_B'$ is the enthalpy change without a buffer contribution, n is the number of protons taken up (positive) or released (negative) upon complex formation, and ΔH_{ion} is the enthalpy of buffer ionization. We measured ΔH_B in three buffers of known ΔH_{ion} [DMG, $\Delta H_{\text{ion}} = -2.5$ kcal mol⁻¹ (38); MES, $\Delta H_{\text{ion}} = 3.7$ kcal mol⁻¹; and cacodylate, $\Delta H_{\text{ion}} = -0.47$ kcal mol⁻¹ (39)]. Fitting these data to eq 1 gives an n of 0.6, in agreement with the potentiometric results of Mauk et al. (21). Thus, $\Delta H_B'$ at pH 6.0 is 1.5 kcal mol⁻¹ more negative than the ΔH_B values shown in Table 1. At pH 6.5, n is 0.2 (21), making $\Delta H_B'$ 0.5 kcal mol⁻¹ more negative than ΔH_B . At pH 7.0, n equals zero, and there is no contribution from buffer ionization.

An equation analogous to eq 1 can be written to correct ΔC_p for the effect of buffer ionization, but ΔC_p for DMG ionization is unknown. We can, however, estimate a range of reasonable corrections by using the range of known buffer ΔC_p values (39). Specifically, the range of buffer ionization heat capacities is +15 to -45 cal mol⁻¹ K⁻¹ and $n = 0.6$ at pH 6.0. Therefore, the range of correction is +9 to -27 cal mol⁻¹ K⁻¹, smaller than the uncertainty in the binding ΔC_p , 62 cal mol⁻¹ K⁻¹. In summary, the contribution from buffer ionization heat capacity is insignificant.

DISCUSSION

Binding Free Energy and Stoichiometry. ITC provides a direct measure of the enthalpy change upon protein-protein binding. The shape of integrated data (Figure 1) is determined by the equilibrium constant for the reaction. Thus, by fitting experimental data to a model (32), the binding constant, K_B , and the stoichiometry, N , can be obtained. ΔG_B and ΔS_B are determined by using the relationship $\Delta G_B = -RT \ln K_B$ and the Gibbs equation. Both 1:1 and 2:1 binding models were tested, but we found no evidence to support 2:1 binding. Since ITC requires enough binding heat to obtain a signal, under the conditions used here, we would not detect a second binding site if the absolute value of its ΔH_B is $\lesssim 0.5$ kcal mol⁻¹ or its K_B is $\lesssim 10^4$ M⁻¹. As shown in Table 2, our ΔG_B values agree with those obtained with other techniques under similar conditions.

Table 2: Binding Free Energies for yCc/CcP Complexes

proteins	pH	buffer/temp (°C)	ΔG_B (kcal mol ⁻¹)
Cc/CcP ^a	6.0	50 mM DMG/25	-8.1
Cc/Zn-CcP ^b	7.0	50 mM KP ₄ /20	-7.8
Cc/CcP ^c	6.0	100 mM KNO ₃ /25	-8.5
Ru-39-Cc/CcP ^d	7.0	100 mM NaCl/25	-8.3

^a This work. ^{b-d} Data from references 24, 21, and 62, respectively.

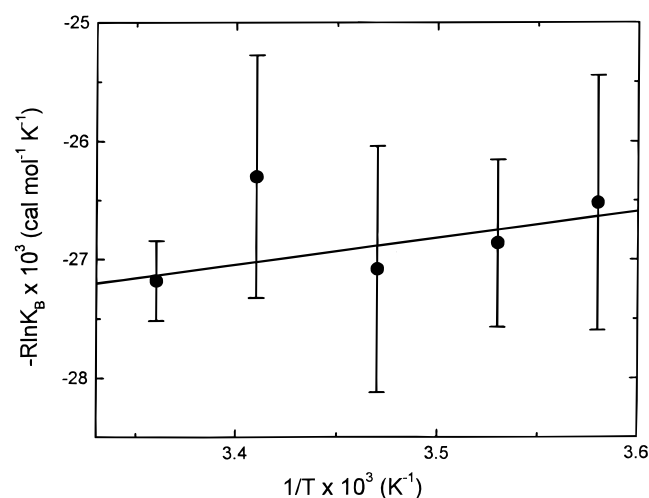


FIGURE 2: Effect of temperature on the binding constant of the yCc/CcP reaction. Experiments were performed at pH 6.0 in 50 mM DMG. The error bars represent the standard deviations of the mean for three to five repetitions. Weighted linear fitting yields a slope of 2.3 ± 1.6 kcal mol⁻¹.

The ionic strength dependence also agrees with earlier work, showing that ionic interactions play an important role in complex formation (21, 24). The product of the charges of Cc and CcP is obtained from the ionic strength dependence (Table 1) and Debye-Hückel limiting law. We obtained a value of -28 ± 7 , which agrees with the Cc and CcP charges of +6 and -4 at pH 6, respectively, as estimated from proton titration curves (40, 41).

Binding Enthalpy. The binding of this physiological heme protein complex is exothermic under all conditions, and mostly enthalpy-driven at 25 °C and 50 mM buffer concentration (Table 1). However, ΔG_B becomes more negative with increasing temperature. This leads to a discrepancy between van't Hoff and calorimetric enthalpies.

The van't Hoff enthalpy of binding, ΔH_{vH} , is calculated from the temperature dependence of the binding constant K_B , by using the integrated van't Hoff equation:

$$\ln K_B = \ln A - \Delta H_{vH}/RT \quad (2)$$

where A is related to the entropy change, R is the gas constant, and T is the absolute temperature.

As shown in Figure 2, a weighted linear fit of a $-R \ln K_B$ versus $1/T$ plot of yCc/CcP binding yields a ΔH_{vH} of 2.3 ± 1.6 kcal mol⁻¹. ΔH_{vH} differs from ΔH_B in both magnitude and sign. Using pH-stat measurements, Mauk et al. estimate a ΔH_{vH} of 0.2 ± 0.8 kcal mol⁻¹ (21), which is also inconsistent with our calorimetric values. These analyses assume that ΔH_{vH} is temperature-independent (i.e., ΔC_p is zero), an assumption that our data show to be incorrect. Nevertheless, the local slope of the plot in Figure 2 shows that ΔH_{vH} is always positive while the data in Table 1 show

that ΔH_B is always negative. Differences between van't Hoff and calorimetric enthalpy changes have been reported for protein-protein, protein-ligand, and protein-DNA binding reactions (42-50).

What are the reasons for the discrepancy between ΔH_B and ΔH_{vH} for yCc/CcP complex formation? As discussed by Stites (51), ITC gives the global enthalpy change, but our van't Hoff analysis assumes a simple 1:1 binding model and ignores potential contributions from other processes linked to complex formation. Such processes include heats of proton uptake or release (eq 1), differences in the Donnan nonideality (52), protein conformational changes, and reorganization of solvent. These processes are not written into the equilibrium constant of eq 2, so they are not reflected in ΔH_{vH} .

Here we consider each of these factors. A 1:1 binding model is appropriate since all our data are well fit by a one-site model but poorly fit by a two-site model, and the fitted stoichiometry is 1:1 (Table 1). The heat of proton release, discussed above, cannot account for the difference. To test the effects of Donnan nonideality, we performed a series of ITC experiments to obtain ΔH_{vH} at a higher ionic strength (100 mM DMG, data not shown). If the Donnan nonideality were a significant factor, we would expect the discrepancy between ΔH_{vH} and ΔH_B to decrease at higher ionic strength, but the opposite was observed. Comparing the crystal structures of Cc, CcP, and the complex indicates little conformational change upon complex formation (8). Since none of these effects appear to be significant, we are left with solvent reorganization in an intermediate state not accounted for in our simple model. Such reorganization has been shown to contribute several kilocalories per mole to ΔH_B (48, 49, 53, 54).

Binding Entropy. ΔS_B is positive under most conditions (Table 1). The binding entropy is even larger if we use ΔH_{vH} . Therefore, the entropy decrease caused by two protein particles going to one complex particle is more than offset by entropy increases caused by other processes. This observation is also consistent with the idea of solvent reorganization upon complex formation. The entropy contribution for removing one bound water molecule is 0-2 kcal mol⁻¹ at 300 K (55).

Surface Area Change and ΔC_p , ΔH_B Estimation. Several relationships between the solvent-accessible surface area buried upon complex formation and ΔH_B and ΔC_p have been proposed. Using the crystal structure of the yCc/CcP complex and the program GEPOL, we calculated that 608 Å² of polar and 646 Å² of apolar SASA are buried upon formation of the complex. However, the apolar SASA change ($\Delta \text{SASA}_{\text{apolar}}$) is a lower estimate because the methyl groups of trimethyl Lys72 of yCc, although close to the binding site, are not observed in the crystal structure of the complex. Assuming the methyl group is completely buried upon binding, we obtained a $\Delta \text{SASA}_{\text{apolar}}$ of 751 Å². Therefore, we use 646 and 751 Å² as the lower and upper limits for $\Delta \text{SASA}_{\text{apolar}}$.

Murphy and Freire (56) estimate ΔC_p from the equation:

$$\Delta C_p = 0.45 \Delta \text{SASA}_{\text{apolar}} - 0.26 \Delta \text{SASA}_{\text{polar}} \quad (3)$$

Spolar et al. (35) propose another approach using only $\Delta \text{SASA}_{\text{apolar}}$:

$$\Delta C_p = 0.25 \Delta \text{SASA}_{\text{apolar}} \quad (4)$$

Table 3: Comparison of yCc/CcP and hCc/CcP Complexes^a

parameter	yCc/CcP	hCc/CcP ^b
$\Delta S_{ASA_{apol}}$	646–751	593
$\Delta S_{ASA_{pol}}$	608	470
ΔC_p , obsd	-216 ± 62	-28 ± 10
ΔC_p , eq 3	-133 to -180	-145
ΔC_p , eq 4	-162 to -187	-148
ΔH_B , obsd	-6.2 ± 0.3	$+2.84 \pm 0.26$
ΔH_B , eq 5	-11.3 to -6.5	-5.60
ΔH_B , eq 6	-10.0 to -10.9	-8.90

^a The units for ΔS_{ASA} , ΔC_p , and ΔH are \AA^2 , $\text{cal mol}^{-1} \text{K}^{-1}$, and kcal mol^{-1} , respectively. ^b From reference 22.

As shown in Table 3, these equations yield ΔC_p estimates that are in reasonable agreement with the measured value, $-216 \pm 62 \text{ cal mol}^{-1} \text{K}^{-1}$.

ΔH_B can be estimated from eq 5 (56):

$$\Delta H_B = 35\Delta S_{ASA_{polar}} - \Delta T\Delta C_p \quad (5)$$

where ΔT is 100 minus the temperature of interest in degrees centigrade. The range of values in Table 3 was obtained by using a temperature of 25 °C and both the measured ΔC_p and the ΔC_p values obtained from eq 3. Weber developed another approach based on the exclusion of water molecules upon complex formation (57):

$$\Delta H_B = (\Delta H_{ww} + \Delta H_{pp} - 2\Delta H_{pw}) \times n_w \quad (6)$$

where ΔH_{ww} , ΔH_{pp} , and ΔH_{pw} are the enthalpy changes for interactions at the solvent–solvent, protein–protein, and protein–solvent interfaces (-7000 , -760 , and -3840 cal/mol , respectively). n_w , the number of water molecules excluded from the binding interface upon complex formation, is estimated by dividing the total surface area change upon complex formation by the surface area of a water molecule, 10 \AA^2 . The range of ΔH_B values calculated is given in Table 3.

In general, the ΔH_B values from eqs 5 and 6 are more exothermic than the measured values. The differences between the calculated and observed values for both ΔC_p and ΔH_B are probably the result of the strong ionic interactions at the binding interface, which are not considered in the model studies used to develop the equations.

Comparison with hCc/CcP. ΔG_B for the intraspecies complex (yCc/CcP) is 1.4 – $2.7 \text{ kcal mol}^{-1}$ more favorable than ΔG_B for the interspecies complex (hCc/CcP) (22), consistent with the results from a previous study (24).

The measured ΔH_B and ΔC_p for complex formation between yCc and CcP (Table 1) are also different from those for the formation of the hCc/CcP complex (Table 3). yCc/CcP binding is exothermic and becomes more exothermic with increasing ionic strength, but hCc/CcP binding is endothermic with a ΔH_B of $\sim 2.4 \text{ kcal mol}^{-1}$ (22), which is independent of ionic strength. ΔC_p for yCc/CcP binding is $-216 \text{ cal mol}^{-1} \text{K}^{-1}$ while ΔC_p for hCc/CcP binding is $-28 \text{ cal mol}^{-1} \text{K}^{-1}$ (22). Importantly, ΔH_B and ΔC_p for yCc/CcP complex formation are in reasonable agreement with the calculated values, unlike the observed and calculated values for hCc/CcP binding (Table 3).

These observations suggest that the crystal structure of the yCc/CcP complex is the same as the solution structure, in agreement with previous studies of electron-transfer

kinetics (58–60). However, the data for the hCc/CcP complex suggest that the crystal and solution structures of the complex and solution are different, consistent with a recent electron-transfer kinetics study (61).

Effect of Reducing the Cc Heme. ΔG_B and ΔH_B for ferro-Cc/CcP binding are less favorable than those for ferri-Cc/CcP binding (Table 1). This result can be partly explained by the fact that ferro-Cc has one less positive charge than does ferri-Cc. It is interesting to compare ΔH_B of ferro-Cc/CcP binding to the calculated values in Table 3. That is, the differences between the measured and calculated values are greater for ferro-Cc/CcP complex formation. This observation leaves open the possibility that the agreement between the calculated and observed values for ferri-Cc/CcP complex is fortuitous.

SUMMARY

In the present investigation, we performed equilibrium thermodynamic studies on yCc/CcP complex formation using ITC. The binding free energy, ranging from -7.4 to $-10.9 \text{ kcal mol}^{-1}$, agrees with results obtained from other techniques. Both enthalpy and entropy favor binding. Measured enthalpy and heat capacity changes are close to the estimated values calculated from binding-induced surface area changes. The van't Hoff enthalpy is different from calorimetric enthalpy, which we suggest is due to a water release step not accounted for in our simple model. Our results also suggest that the solution structure of the yCc/CcP complex is the same as its crystal structure.

ACKNOWLEDGMENT

We thank Brett Terrogowan for help with the calorimeters, Thomas Poulos for supplying the CcP expression system, and the Pielak group and Dorothy Erie for helpful discussions.

REFERENCES

- Goodin, D. B., Mauk, A. G., and Smith, M. (1986) *Proc. Natl. Acad. Sci. U.S.A.* 83, 1295–1299.
- Louie, G. V., and Brayer, G. D. (1990) *J. Mol. Biol.* 214, 527–555.
- Berghuis, A. M., and Brayer, G. D. (1992) *J. Mol. Biol.* 223, 959–976.
- Finzel, B. C., Poulos, T. L., and Kraut, J. (1984) *J. Biol. Chem.* 259, 13027–13036.
- Fitzgerald, M. M., Musah, R. A., McRee, D. E., and Goodin, D. B. (1996) *Nat. Struct. Biol.* 3, 626–631.
- Wang, J., Mauro, M., Edwards, S. L., Oatley, S. J., Fishel, L. A., Ashford, V. A., Xuong, N., and Kraut, J. (1990) *Biochemistry* 29, 7160–7173.
- Goodin, D. B., and McRee, D. E. (1993) *Biochemistry* 32, 3313–3324.
- Pelletier, H., and Kraut, J. (1992) *Science* 258, 1748–1755.
- Beetlestine, J. (1960) *Arch. Biochem. Biophys.* 89, 34–40.
- Mochan, E., and Nicholls, P. (1971) *Biochem. J.* 121, 69–82.
- Dowe, R. J., Vitello, L. B., and Erman, J. E. (1984) *Arch. Biochem. Biophys.* 232, 566–573.
- Kang, C. H., Ferguson-Miller, S., and Margoliash, E. (1977) *J. Biol. Chem.* 252, 919–926.
- Kornblatt, J. A., and English, A. M. (1986) *Eur. J. Biochem.* 155, 505–511.
- Erman, J. E., and Vitello, L. B. (1980) *J. Biol. Chem.* 255, 6224–6227.
- Yi, Q., Erman, J. E., and Satterlee, J. D. (1993) *Biochemistry* 32, 10988–10994.
- Yi, Q., Erman, J. E., and Satterlee, J. D. (1994) *Biochemistry* 33, 12032–12041.

17. Jeng, M.-F., Englander, S. W., Pardue, K., Rogalskyj, J. S., and McLendon, G. (1994) *Nat. Struct. Biol.* 1, 234–238.
18. Sukits, S. F., Erman, J. E., and Satterlee, J. D. (1997) *Biochemistry* 36, 5251–5259.
19. Vitello, L. B., and Erman, J. E. (1987) *Arch. Biochem. Biophys.* 258, 621–629.
20. Corin, A. F., McLendon, G., Zhang, Q., Hake, R. A., Falvo, J., Lu, K. S., Ciccarelli, R. B., and Holzschu, D. (1991) *Biochemistry* 30, 11585–11595.
21. Mauk, M. R., Ferrer, J. C., and Mauk, A. G. (1994) *Biochemistry* 33, 12609–12614.
22. Kresheck, G. C., Vitello, L. B., and Erman, J. E. (1995) *Biochemistry* 34, 8398–8405.
23. Erman, J. E., Kresheck, G. C., Vitello, L. B., and Miller, M. A. (1997) *Biochemistry* 36, 4054–4060.
24. Stemp, E. D. A., and Hoffman, B. M. (1993) *Biochemistry* 32, 10848–10865.
25. Zhou, J. S., and Hoffman, B. M. (1993) *J. Am. Chem. Soc.* 115, 11008–11008.
26. Zhou, J. S., and Hoffman, B. M. (1994) *Science* 265, 1693–1696.
27. Cutler, R. L., Pielak, G. J., Mauk, A. G., and Smith, M. (1987) *Protein Eng.* 1, 95–99.
28. Gao, Y., Boyd, J., Pielak, G. J., and Williams, R. J. P. (1991) *Biochemistry* 30, 1928–1934.
29. Willie, A., McLean, M., Liu, R. Q., Hilgen-Willis, S., Saunders, A. J., Pielak, G. J., Sligar, S. G., Durham, B., and Millett, F. (1993) *Biochemistry* 32, 7519–7525.
30. Fisher, L. A., Villafranca, J. E., Mauro, M., and Kraut, J. (1987) *Biochemistry* 26, 351–360.
31. Dasgupta, S., Rousseau, D. L., Anni, H., and Yonetani, T. (1989) *J. Biol. Chem.* 264, 654–662.
32. Bevington, P. R. (1969) *Data Reduction and Error Analysis in the Physical Sciences*, McGraw-Hill, New York.
33. Silla, E., Tuñón, I., and Pascual-Ahuir, J. L. (1991) *J. Comput. Chem.* 12, 1077–1088.
34. Lee, B., and Richards, F. M. (1971) *J. Mol. Biol.* 55, 379–400.
35. Spolar, R. S., Livingstone, J. R., and Record, M. T., Jr. (1992) *Biochemistry* 31, 3947–3955.
36. Wiseman, T., Williston, S., Brandts, J. F., and Lin, L. N. (1989) *Anal. Biochem.* 179, 131–137.
37. Dawson, R. M. C., Elliott, D. C., Elliott, W. H., and Jones, K. M. (1959) *Data For Biochemical Research*, Clarendon, Oxford.
38. Jones, I., and Soper, F. G. (1936) *J. Chem. Soc.*, 133–137.
39. Fukada, H., and Takahashi, K. (1998) *Proteins: Struct., Funct., Genet.* 33, 159–166.
40. Conroy, C. W., and Erman, J. E. (1978) *Biochim. Biophys. Acta* 537, 396–405.
41. Barker, P. D., Mauk, M. R., and Mauk, A. G. (1991) *Biochemistry* 30, 2377–2383.
42. Mukkur, T. K. S. (1984) *CRC Crit. Rev. Biochem.* 16, 133–167.
43. Wiesinger, H., and Hinz, H.-J. (1986) *Thermodynamic Data for Biochemistry and Biotechnology*, Springer-Verlag, Berlin.
44. Sigurskjold, B. W., and Bundle, D. R. (1992) *J. Biol. Chem.* 267, 8371–8376.
45. De Cristofaro, R., and Landolfi, R. (1994) *J. Mol. Biol.* 239, 569–577.
46. Gilli, P., Ferreti, V., Gilli, G., and Borea, P. A. (1994) *J. Phys. Chem.* 98, 1515–1518.
47. Sigurskjold, B. W., Berland, C. R., and Svensson, B. (1994) *Biochemistry* 33, 10191–10199.
48. Naghbi, H., Tamura, A., and Sturtevant, J. M. (1995) *Proc. Natl. Acad. Sci. U.S.A.* 92, 5597–5599.
49. Liu, Y., and Sturtevant, J. M. (1995) *Protein Sci.* 4, 2559–2561.
50. Færgeman, N. J., Sigurskjold, B. W., Kragelund, B. B., Andersen, K. V., and Knudsen, J. (1996) *Biochemistry* 35, 14118–14126.
51. Stites, W. E. (1997) *Chem. Rev.* 97, 1233–1250.
52. Tanford, C. (1961) *Physical Chemistry of Macromolecules*, John Wiley & Sons, New York.
53. Connelly, P. R., Thomson, J. A., Fitzgibbon, M. J., and Bruzzese, F. J. (1993) *Biochemistry* 32, 5583–5590.
54. Chervenak, M. C., and Toone, E. J. (1994) *J. Am. Chem. Soc.* 116, 10533–10539.
55. Dunitz, J. D. (1994) *Science* 264, 670–670.
56. Murphy, K. P., and Freire, E. (1992) *Adv. Protein Chem.* 43, 313–361.
57. Weber, G. (1993) *J. Phys. Chem.* 97, 7108–7115.
58. Miller, M. A., Geren, L., Han, G. W., Saunders, A., Beasley, J., Pielak, G. J., Durham, B., Millett, F., and Kraut, J. (1996) *Biochemistry* 35, 667–673.
59. Pappa, H. S., Tajbaksh, S., Saunders, A. J., Pielak, G. J., and Poulos, T. L. (1996) *Biochemistry* 35, 4837–4845.
60. Wang, K., Mei, H., Geren, L., Miller, M. A., Saunders, A., Wang, X., Waldner, J. L., Pielak, G. J., Durham, B., and Millett, F. (1996) *Biochemistry* 35, 15107–15119.
61. Mei, H., Wang, K., Peffer, N., Weatherly, G., Cohen, D. S., Miller, M., Pielak, G., Durham, B., and Millett, F. (1999) *Biochemistry* 38, 6846–6854.
62. Mei, H., Wang, K., McKee, S., Wang, X., Waldner, J. L., Pielak, G. J., Durham, B., and Millett, F. (1996) *Biochemistry* 35, 15800–15806.

BI992005I